IMPEDANCE MATCHED MASS-DAMPERS:A NEW APPROACH FOR IMPROVING STRUCTURAL DAMPING

Craig Gardner, General Electric-Power Generation[1]
Richard H. Lyon, MIT

ABSTRACT

Statistical Energy Analysis (SEA) techniques are used to analytically determine the damping effect achieved by attaching a quantity of mass-dampers to a damped flat plate. Mass-dampers are defined as SDOF oscillators which are over damped and have a resonant frequency below the frequency range of interest. The analysis has shown that the damping effect achieved by this approach is maximized when damper impedance is matched to a particular ratio of the average drive point impedance of the plate. The analysis indicates that the damping effect achieved is significant for mass-damper mass to plate mass ratios as low as 0.05 to 0.2.

A prototype mass-damper system was designed and tested to verify the analytical results. The experimental results showed that significant improvements in damping were achieved and that the amplitude of modal frequencies were reduced by as much as 10-15 dB over a wide frequency range.

This approach differs from visco-elastic techniques in that it does not share strain energy with base structure. This characteristic may make this approach effective for damping stiff structures at low frequencies.

[1] 1100 Western Ave., Lynn MA 01910, MS:GPNR7, Tel.(617) 594-6241

1.0 INTRODUCTION

The low frequency damping characteristics of many structures are critical to their performance. Among such structures are submarines, which must have low structureborne noise levels to remain undetected and tall buildings which need to minimize wind induced and seismic vibrations for comfort and safety considerations. Other applications may include reducing low frequency vibrations in aircraft and automobiles to improve passenger comfort.

Designing and implementing structural damping systems which perform well on stiff structures at low frequencies is a challenging task. Visco-elastic materials are often used in the design of such damping systems. In order for such designs to be effective, they must share a significant portion of the dynamic strain energy. This requirement can at times be difficult to obtain in practice.

Because of this difficulty, a damping system which did not rely on sharing strain energy with the base structure might have an advantage. Such a system would ideally function over a broad frequency range and not be tuned to a particular resonance of the base structure as is the case with tuned absorbers.

Our approach began by analyzing the effect of adding a quantity of masses and a dashpots combined in series on plate dynamics. Figure 1 shows a plate with 6 Mass-Dampers. It was felt that impedance matching of the Mass-Dampers to the plate could result in dissipating a significant amount of power and therefore increase the damping of the plate.

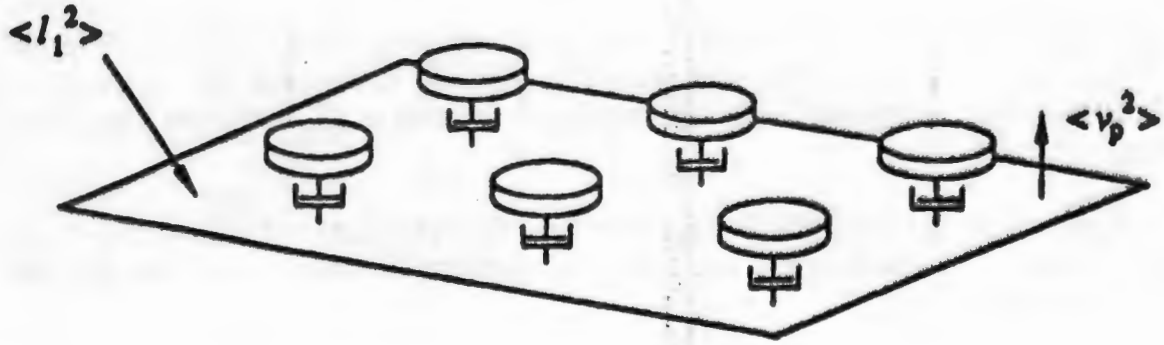

Figure 1 Plate with 6 Mass-Dampers.

Statistical Energy Analysis (SEA) techniques were used to analyze the effectiveness of these Impedance Matched Mass-Dampers. A prototype system of Mass-Dampers was designed based on squeeze film damping principles. The effectiveness of these dampers was experimentally verified and compared with analytical predictions.

2.0 SEA ANALYSIS OF A PLATE WITH MASS-DAMPERS

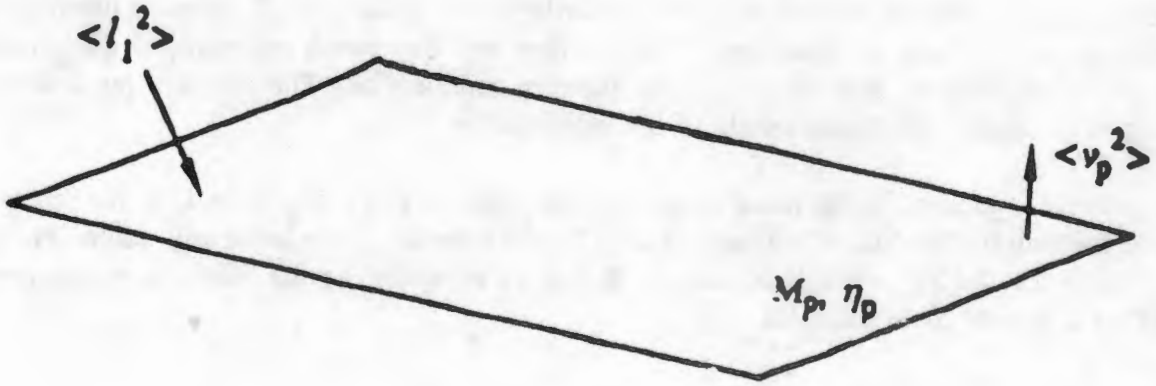

Figure 2 Rectangular plate with mean-square input force $<l_1^2>$, average m.s. velocity $<v_p^2>$, drive point conductance G_p, loss factor η_p, and mass M_p.

Lyon[1] has shown that for the plate shown on Fig. 2 the power input to the plate and dissipated by the plate are equal and therefore the average mean-square transfer function TF is given by eq. (1).

$$\frac{<v_p^2>}{<l_1^2>} = \frac{\overline{G_p}}{\omega \eta_p M_p} \tag{1}$$

where:

$<v_p^2>$ = average mean square plate velocity
$<l_1^2>$ = average mean square input force
$\overline{G_p}$ = average plate drive point conductance = Real part of plate mobility
$\omega \eta_p M_p$ = R_p = effective plate resistance
η_p, M_p = plate loss factor and mass respectively

Note that the basic form for the plate TF is a ratio of the plate conductance to the plate resistance, R_p.

We expand on this concept to derive an expression for the plate TF with mass-dampers. Fig. 3 shows the system which we will analyze, a plate with two Mass-Dampers. The mass-dampers shown on Fig. 3 are basically SDOF systems that have the same components as a tuned damped absorber.

Our approach to using these elements will be different from the tuned damped absorber approach in two important aspects. First, these mass-dampers are designed to improve structural damping

at frequencies well above their undamped natural frequency by using an impedance matching approach. Tuned absorbers are frequency tuned to add damping for a particular structural mode.

Second, these mass-dampers are very much overdamped (typical $\zeta = 1.2$) whereas tuned damped absorbers are typically underdamped. Because they are very much overdamped they could be accurately modeled as a simple mass and damper combination. The primary purpose of the spring is to support the static weight of the mass-damper mass.

We derive an equation for the mean square transfer function (TF) $<v_p^2>/<l_1^2>$ for this system where the number of Mass-Dampers, N is 2 but in general N can have any value. From the expression for the TF we will be able to derive an equation for the effective resistance, R_{eff} resulting from the mass-dampers.

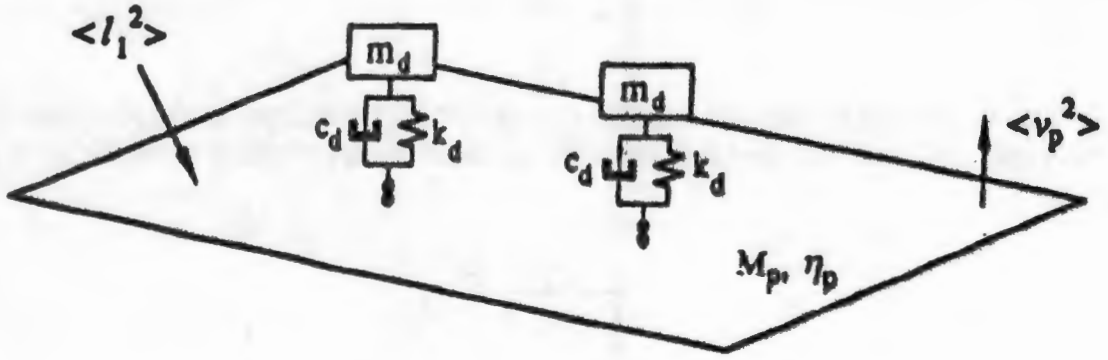

Figure 3 Plate with 2 Mass-Dampers.

We make the following assumptions in performing the analysis:

1. Points on the plate move independently, i.e. the attachment points are separated by a distance greater than half a bending wavelength.

2. The dynamic properties of the plate can be described by average parameters and mean square response.

3. The addition of passive discrete elements does not significantly affect the average drive point conductance of the plate, G_p.

We analyze this system by exercising two reciprocal analytical "experiments". In "experiment 1" as shown in Fig. 4 a mean-square force $<l_1^2>$ is applied to the plate and the points on the plate that attach to the two dampers are "blocked". Forces $<l_{bl13}^2>$ and $<l_{bl11}^2>$ are applied such that the mean square velocities, $<v_{13}^2>$ and $<v_{11}^2>$ at these points are zero. We assume that the system is linear and that locations 11 and 13 are typical and therefore the blocked forces applied at these points are equal.

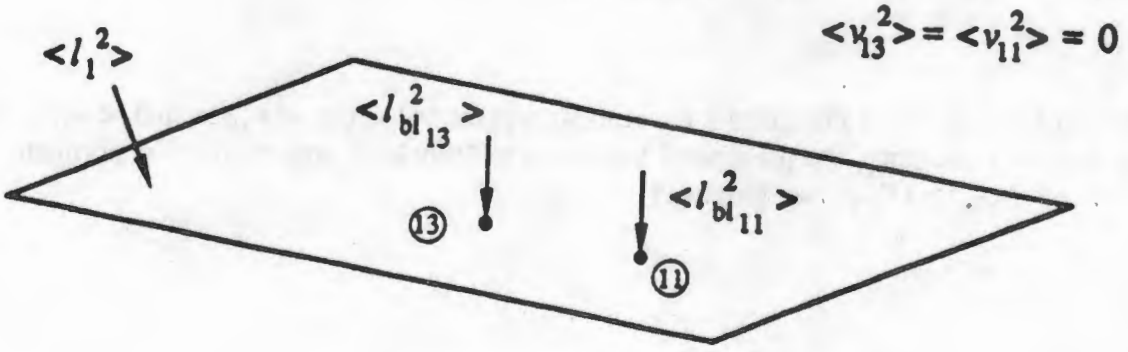

Figure 4 "Experiment 1" with input force $<l_1^2>$ and "blocked" forces $<l_{bl13}^2>$ and $<l_{bl11}^2>$.

We also assume linearity so, that the "blocked" force, $<l_{bl}^2>$ is proportional to the mean square plate velocity, $<v_p^2>$ as shown by eq. (2).

$$<l_{bl}^2> = \Gamma' <v_p^2> \tag{2}$$

Since the power input to the plate equals the power dissipated,

$$\Pi_{in} = \Pi_{dissipated} \tag{3}$$

$$<l_1^2> \overline{G_p} = \omega \eta_p M_p <v_p^2> \tag{4}$$

where:

$\langle I_1^2 \rangle$ = mean square input force
$\overline{G_p}$ = Real Part of plate mobility=$(8\rho_s \kappa c_l)^{-1}$
ρ_s = surface mass density
κ = radius of gyration
h = plate thickness
c_l = longitudinalwave speed
η_p = plate loss factor
M_p = plate mass
$\langle v_p^2 \rangle$ = average m.s. plate velocity over space and time

In "experiment 2" we prescribe 2 equal mean-square velocities $\langle v'^2_{11} \rangle$ and $\langle v'^2_{13} \rangle$ as shown on Figure 5. Relating the prescribed velocities to "blocked" forces from "experiment 1"[2], i.e., $\langle v^2 \rangle = \langle I_{bl}^2 \rangle |Y_{eff}|^2$, we obtain (5).

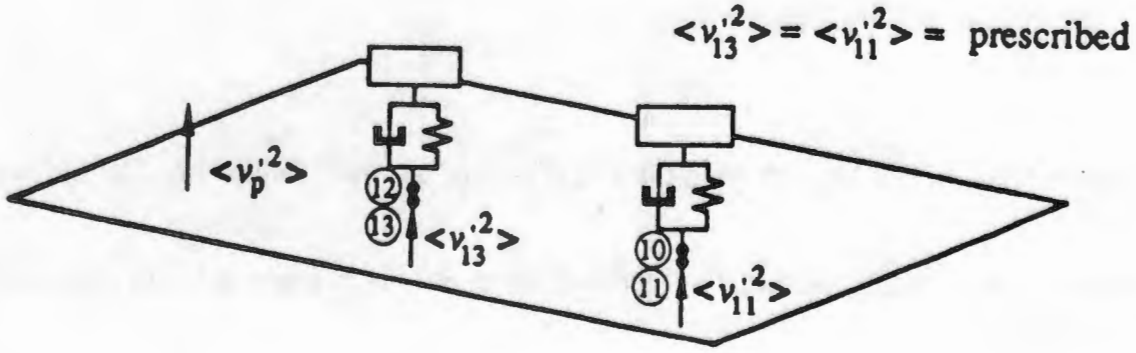

Figure 5 "Experiment 2" with prescribed velocity inputs.

$$\langle v'^2_{10} \rangle = \langle v'^2_{11} \rangle = \frac{\langle I_{bl_{11}}^2 \rangle |Y_{10}|^2 |Y_{11}|^2}{|Y_{10}+Y_{11}|^2} \qquad (5)$$

where:

The mean square plate mobility $|Y_{10}|^2$ is given by[3] as shown in equation (6).

$\langle v'^2_{10} \rangle$ = prescribed velocity at plate - damper junction
Y_{10} = drive point mobility of mass-damper
Y_{11} = drive point mobility of plate

$$|Y_{11}|^2 = \overline{G}_p^2 + \sigma_{\overline{G}_p}^2 + \sigma_{B_p}^2 \tag{6}$$

where:

$\sigma_{\overline{G}_p}^2$ = input conductance variance $= 9\overline{G}_p / 8M$
M = modal overlap $= \Pi f \eta_p / 2\overline{\delta f}$
$\sigma_{B_p}^2$ = input susceptance variance $= \sigma_{\overline{G}_p}^2$
f = frequency (Hz)
$\overline{\delta f}$ = average modal spacing

If we assume that the locations of the mass-dampers are typical and therefore the velocities at the mass-damper plate are the same, then each mass-damper will dissipate the same amount of power. Furthermore, in order for energy to be conserved the power input to a mass-damper must equal the power dissipated by it as shown by equation (7).

$$\langle v'^2_{10} \rangle R_{10} = C_d |v'_{10} - v'_d|^2 \tag{7}$$

where:

R_{10} = $G_{10} / |Y_{10}|^2$ = $\Re$ part of mass-damper drive point impedance
G_{10} = drive point conductance of mass-damper
$|Y_{10}|^2$ = mean square drive point mobility of mass-damper
v'_d = mass-damper mass velocity
C_d = damper constant

The power input and dissipated by the plate is given by equation (8).

$$N \langle v'^2_{11} \rangle R_{11} = \omega \ \eta_p \ M_p \langle v_p^2 \rangle \tag{8}$$

By reciprocity[2] the ratio of the input force to the blocked force of "experiment 1" is equal to the ratio of the prescribed velocity to the mean square plate velocity of "experiment 2" as shown by equation (9).

$$\frac{\langle I_1^2 \rangle}{\langle I_{b1}^2 \rangle} = \frac{\langle v'^2_{10} \rangle}{\langle v'^2_p \rangle} \tag{9}$$

Substituting equations (2),(4) and (8) in (9) and we get (10).

$$\Gamma' = \frac{R_{11}}{\overline{G_p}} = \frac{1}{|Y_{11}|^2} \tag{10}$$

We can now get an expression for the plate velocity at the mass-damper plate junction, v'_{11} in terms of the "free" plate velocity, v_p by substituting (2), (5) and (8) in equation (10) which yields (11).

$$\frac{\langle v'^2_{11} \rangle}{\langle v_p^2 \rangle} = \frac{|Y_{10}|^2}{|Y_{10}+Y_{11}|^2} \tag{11}$$

It can be shown[4] that by considering v_{10} to be a velocity source applied to the mass-damper oscillator then the relative velocity across the damper can be defined in terms of the mass-damper mobilities and the junction velocity as shown by equation (12).

$$v_{10} - v_d = v_{10}\left[\frac{Y_{kd}Y_{cd}}{(Y_{kd}Y_{cd})+Y_{md}(Y_{kd}+Y_{cd})}\right] \tag{12}$$

where:

v_{10} = velocity at plate, mass-damper junction
v_d = mass-damper mass velocity
Y_{cd} = mobility of mass-damper damper
Y_{kd} = mobility of mass-damper spring
Y_{md} = mobility of mass-damper mass

We will now use these results to determine the mean-square transfer mobility for a plate with N mass-dampers. Since the system is conservative,

$$\Pi_{input} = \Pi_{diss.\ plate} + \Pi_{diss.\ mass\text{-}dampers} \tag{13}$$

The input power is simply the product of the plate drive point conductance and the mean square input force as shown by eq. (14).

$$\Pi_{input} = \langle l_1^2 \rangle \overline{G_p} \tag{14}$$

The power dissipated by the plate is given by eq. (15) and is equal to the effective resistance of the plate times the mean-square plate velocity.

$$\Pi_{diss.\ plate} = \omega \eta_p M_p \langle v_p^2 \rangle \tag{15}$$

The power dissipated by the mass-dampers is equal to the product of the number of mass-dampers, N the damper resistance and the relative mean-square velocity across the damper as shown by eq.(16).

$$\Pi_{diss.\ mass\text{-}dampers} = NC_d |v_{10} - v_d|^2 \tag{16}$$

If we can now combine the results from eqs. (11)-(16) to solve for the average mean-square transfer function for a plate with *N* mass-dampers which is given by eq. (17).

$$\frac{\langle v_p^2 \rangle}{\langle l_1^2 \rangle} = \frac{\overline{G_p}}{\omega \eta_p M_p + NC_d \left[\frac{|Y_{10}|^2 |Y_{kd}|^2 |Y_{cd}|^2}{|Y_{10}+Y_{11}|^2 |Y_{kd}Y_{cd} + Y_{md}(Y_{kd}+Y_{cd})|^2} \right]} \tag{17}$$

It can be seen from eq. (17) that the TF for a plate with mass-dampers has a similar form to that for the plate alone eq. (1), i.e. ratio of conductance to resistance, the only difference being the additional term in the denominator of (17) which is the effective resistance of the mass-dampers. Consequently, eq.(17) can be written in the form shown by eq. (18).

$$\frac{\langle v_p^2 \rangle}{\langle l_1^2 \rangle} = \frac{\overline{G_p}}{R_p + R_{eff}} \tag{18}$$

where:

$$R_p = \omega \eta_p M_p$$

$$R_{eff} = NC_d \left[\frac{|Y_{10}|^2 |Y_{kd}|^2 |Y_{cd}|^2}{|Y_{10}+Y_{11}|^2 |Y_{kd}Y_{cd} + Y_{md}(Y_{kd}+Y_{cd})|^2} \right]$$

We define the η_{eff} as shown in equation (19).

$$\eta_{eff} = \frac{R_{eff}}{\omega M_p} \tag{19}$$

Several FORTRAN programs were then written to evaluate the expressions derived here. The results are discussed in the following section.

3.0 DISCUSSION OF ANALYTICAL RESULTS

We will now look at some of the trends predicted by these analyses. More specifically we will analyze trends predicted for configurations for which we have experimental data.

The plate studied was 1/8 in. (3mm) thick aluminum 24 in. (.61m) wide by 30 in. (.76m) long. It was partially covered with a free layer visco-elastic damping treatment and had an initial average loss factor of .007 over a frequency range of 300-2500 Hz. We studied this plate with 0, 10, 25 and 35, 20 gram mass-dampers.

The plate weighed approximately 4 kg. and the mass dampers added were from 5 to 20% of the plate mass. For the 35 mass-damper system we evaluated the effect of varying the damper constant, C_d on system performance. Because we were primarily interested in the 500-2500 Hz frequency range, the mass-damper natural frequency was set to 40 Hz.

Figure 6 shows the magnitude of the average acceleration/force TF versus the ratio of the mass-damper resistance, C_d to the Real part of the plate impedance, $Re\{Z_p\}$. These calculations are for frequencies ranging from 500 to 10,000 Hz.

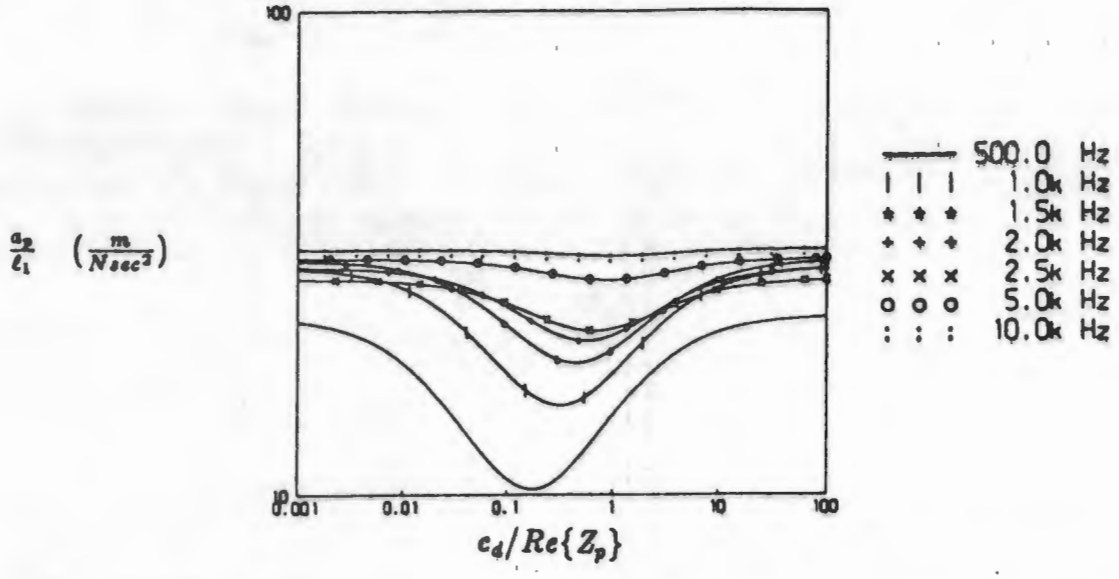

Figure 6 TF vs. $C_d/Re\{Z_p\}$ for plate with 10 mass-dampers evaluated at several frequencies.

It can be seen from Fig. 6 that there is an optimum ratio for which the transfer function response is minimized and that the optimum value increases with frequency. As one might expect with either too low or too high an impedance ratio, the reduction in response is minimal.

This makes sense if we take this concept to extremes. For example if $C_d=0$, there would be no power dissipated by the mass-dampers. On the other hand if $C_d=\infty$ the damper mass would essentially be rigidly attached to the plate and hence would only be adding mass, again with no power dissipation.

It can also be seen from Figure 6 that reduction in the transfer function is most significant at lower frequencies. This data shows that at 500 Hz the magnitude of the TF is reduced $\approx$6dB when the impedance ratio is optimized. Calculations using eq. (17) showed that if we rigidly attach 10 mass-dampers (5% plate mass) we would only expect about a 0.2 dB decrease in the TF at 500 Hz.

Figures 7 and 8 show the TF magnitude vs. impedance ratio for 25 and 35 mass-dampers respectively. Theses curves show the same trends as the 10 mass-damper case but with a stronger effect as the number of mass-dampers is increased. With 35 mass-dampers the optimum

impedance ratio reduces the average TF by 10 dB. The optimum impedance ratio does not change significantly as the number of mass-dampers is increased.

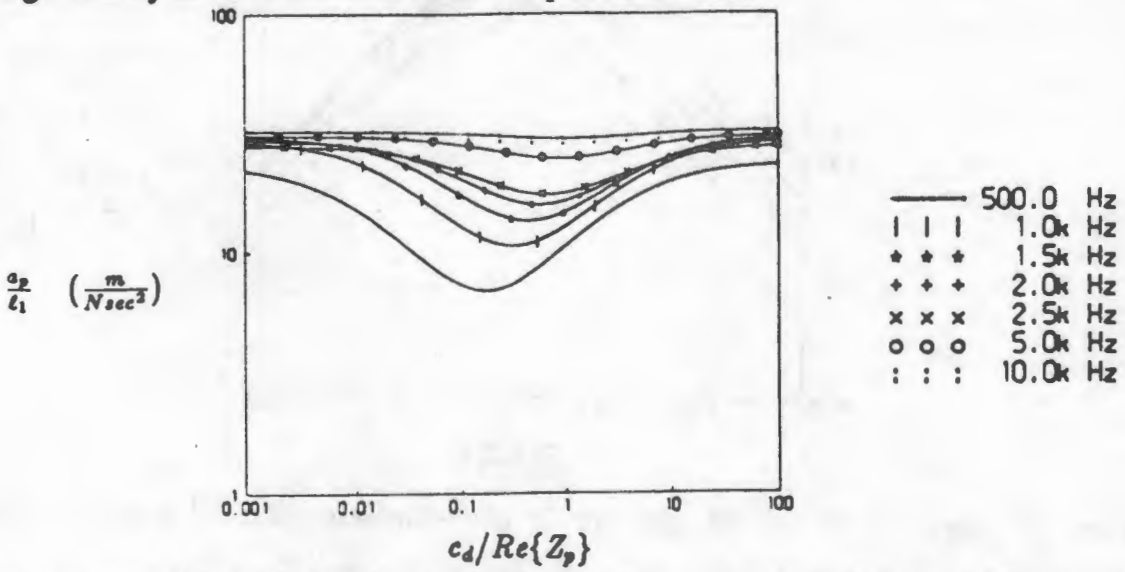

Figure 7 TF vs. Cd/Re{Zp} for plate with 25 mass-dampers evaluated at several frequencies.

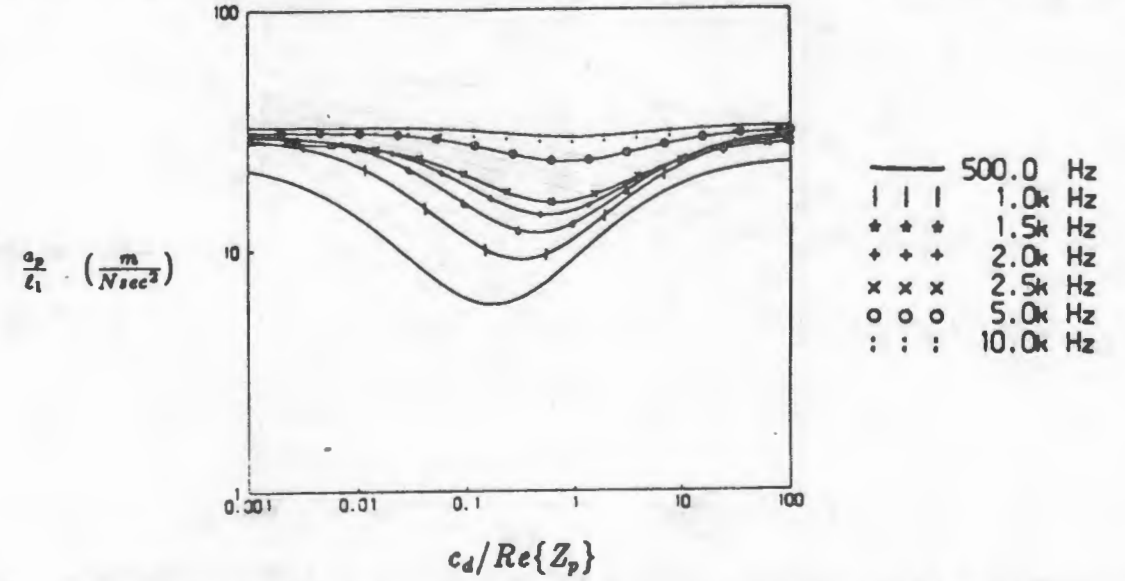

Figure 8 TF vs. Cd/Re{Zp} for plate with 35 mass-dampers evaluated at several frequencies.

Figure 9 shows η_{eff} as defined by eq. (19) as a function of the impedance ratio for 35 mass-dampers. These curves show that loss factors greater than 0.05 are achieved from 500-2000 Hz. It can also be seen from these curves that considering the log scale of the x axis, there is a fairly broad range of impedance ratios for which the η_{eff} is nearly maximized.

If we choose C_d so that the damping by the mass-dampers is maximized at 1000 Hz and plot the TF for the plate with visco-elastic material alone, 10, 25 and 35 mass-dampers we obtain the TF curves shown on Figure 10. These curves show results similar to other additive damping treatments in that large improvements are made initially and incrementally smaller improvements are made by adding more mass-dampers. We should note however, that the plate had some damping to begin with and that the improvement in damping attributable to the mass-dampers

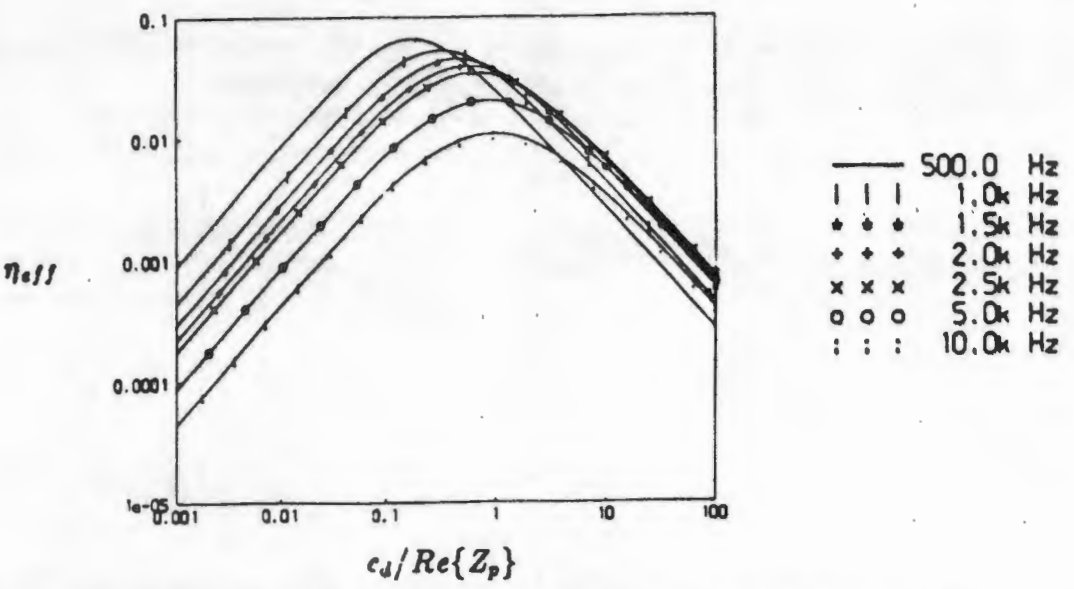

Figure 9 η_{eff} vs. Cd/Re{Zp} for plate with 35 mass-dampers evaluated at several frequencies.

further reduces the TF as much as 10 dB at the lower frequencies.

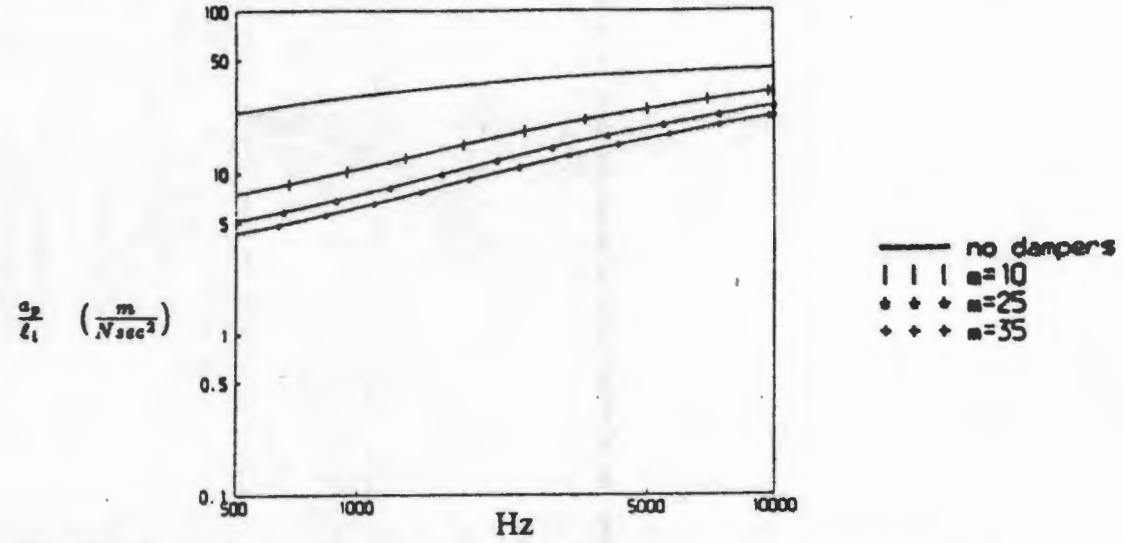

Figure 10 TFs for damped plate alone and with 10, 25, and 35 mass-dampers.

4.0 MASS-DAMPER DESIGN

Visco-elastic materials were originally considered for a prototype mass-damper system but, initial calculations showed that a material with a loss factor of at least 100 would be needed for such a system to work, while present materials have a maximum loss factor of ≈ 1. A fluid film damper approach was chosen because of the simplicity of the design and the large damping constants that can be achieved.It can be shown[5] that the damping resistance for a circular fluid film damper is governed by eq. (20).

$$C_d = \frac{3\pi\mu d^4}{32e^3} \tag{20}$$

where:

C_d= damper constant, $Nsec/m$
μ= dynamic viscosity, $Nsec/m^2$
d= damper diameter
e= film thickness

On Figure 11 can be seen a sketch of the prototype mass-damper system. It consists of an aluminum disk which serves as both the damper mass and the fluid film damper area. The disk diameter was 34mm, chosen so that it is less than 1/2 a bending wavelength on the plate at 2500 Hz. The disk is supported by 3 small cylinders of polyurethane foam whose spring rate was such that the natural frequency of the system was 40 Hz. The polyurethane "springs" were bonded to set screws which were used to vary the film thickness, e and hence the damping constant, C_d. A bead of silicone sealant was used to contain the glycerol. Glycerol was chosen as the damping fluid because of its high dynamic viscosity.

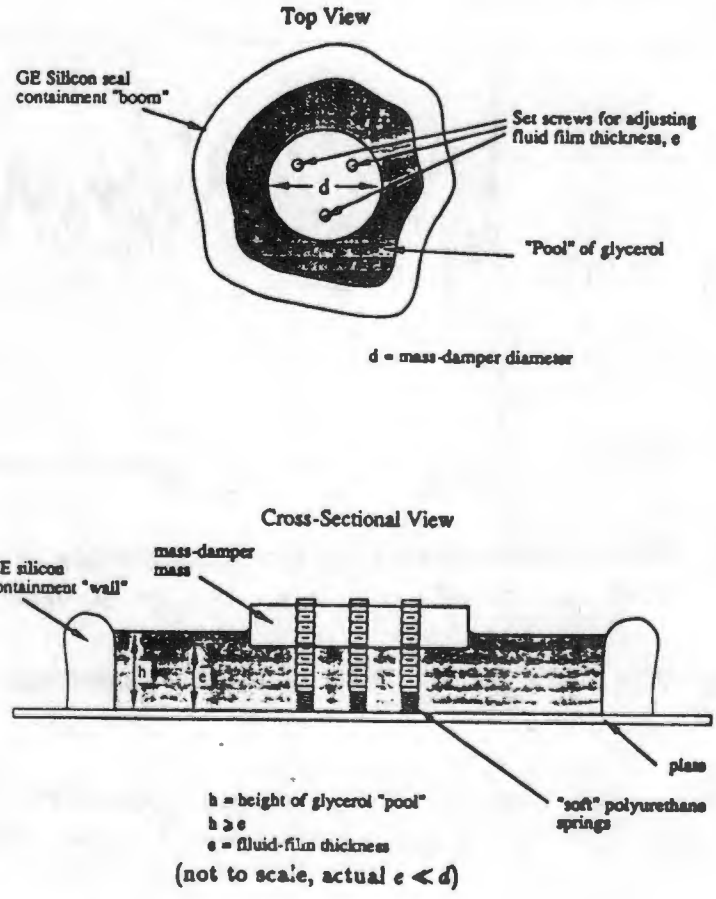

Figure 11 Sketch of fluid film mass-damper design.

5.0 EXPERIMENTAL APPROACH

The experiments were designed to measure the effect of varying the number of mass-dampers and their damping constant, C_d on the average TF and loss factor, η of the plate. A sketch of the experimental setup is shown on Figure 13. The plate was supported by foam rubber to simulate free-free boundary conditions. A 8 channel FFT analyzer was used to measure plate transfer functions for the locations shown on Figure 14 for the 3 different quantities of mass-dampers tested. Average TFs were calculated by averaging the magnitude of the 4 measured frequency response functions using the GenRad signal processing language TSL2. A frequency resolution of 0.25 Hz was used for all measurements. The average loss factor was measured for 4 frequency bands using the integrated impulse technique[6].

6.0 EXPERIMENTAL RESULTS

6.1 EVALUATION OF MASS LOADING EFFECT OF MASS-DAMPERS ON PLATE VIBRATION

Figure 12 shows a comparison of the average TF of the plate with 10 mass-dampers and the average TF of the plate at the mass-damper locations. It can be seen from this figure that the

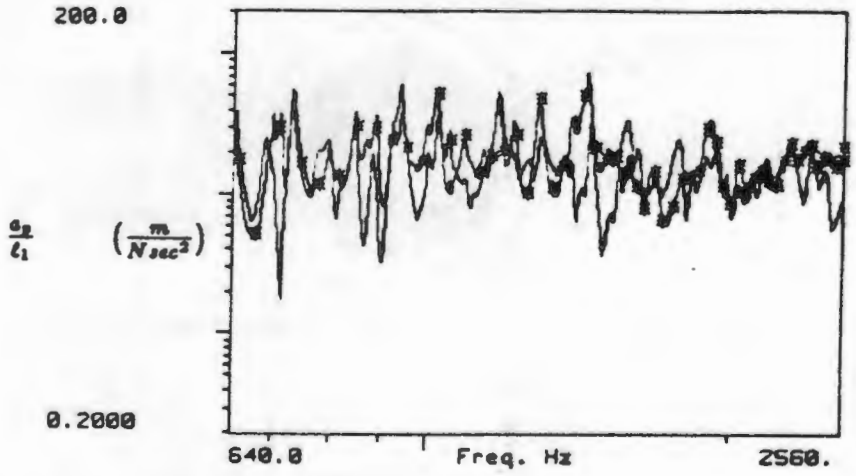

— Average normalized plate acceleration below mass-dampers
*** Average normalized plate acceleration of "free" plate

Figure 12 Comparison of the average "free" plate TF with average TF of the plate below the mass-dampers.

2 curves are quite similar. From this comparison we conclude that the mass-dampers are not mass loading the plate but are acting as a mass damper system as intended.

6.2 EFFECT OF MASS-DAMPERS ON PLATE η AND AVERAGE TF

The analytical data shown in Figure 8 showed that an impedance ratio of 0.32 should minimize the TF at 1000 Hz. This is approximately the mid point of the 0-2500 Hz frequency band of interest. On Table 1 can be seen the estimated plate loss factor, η for 0, 10, 25 and 35 mass-dampers tested with the impedance ratio equal to 0.32. It can be seen from Table 1 that there is a significant increase in the measured plate loss factor as the number of mass-dampers is increased. The increase is on the order of 200-500% and is evident over frequency span of almost 2000 Hz. It should be noted that due to the difficulty of measuring the fluid film thickness of this softly sprung system, the impedance ratios can only be considered approximate.

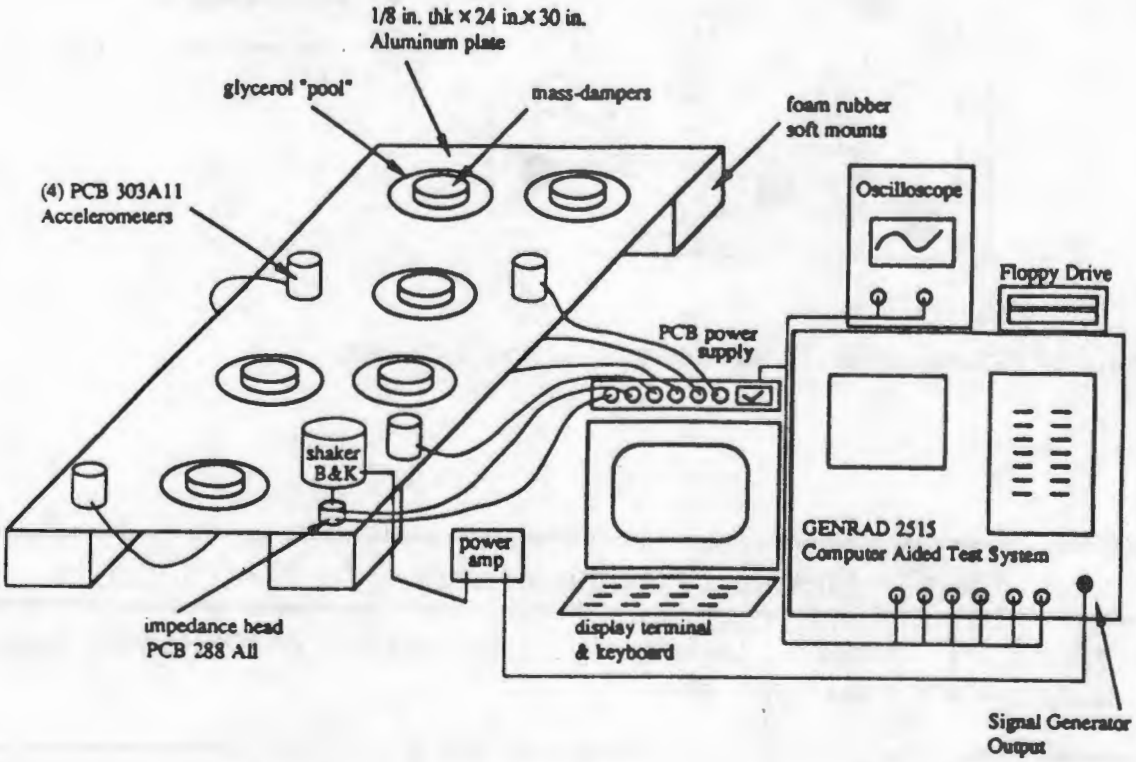

Figure 13 Experimental Set-up for measuring TFs and η.

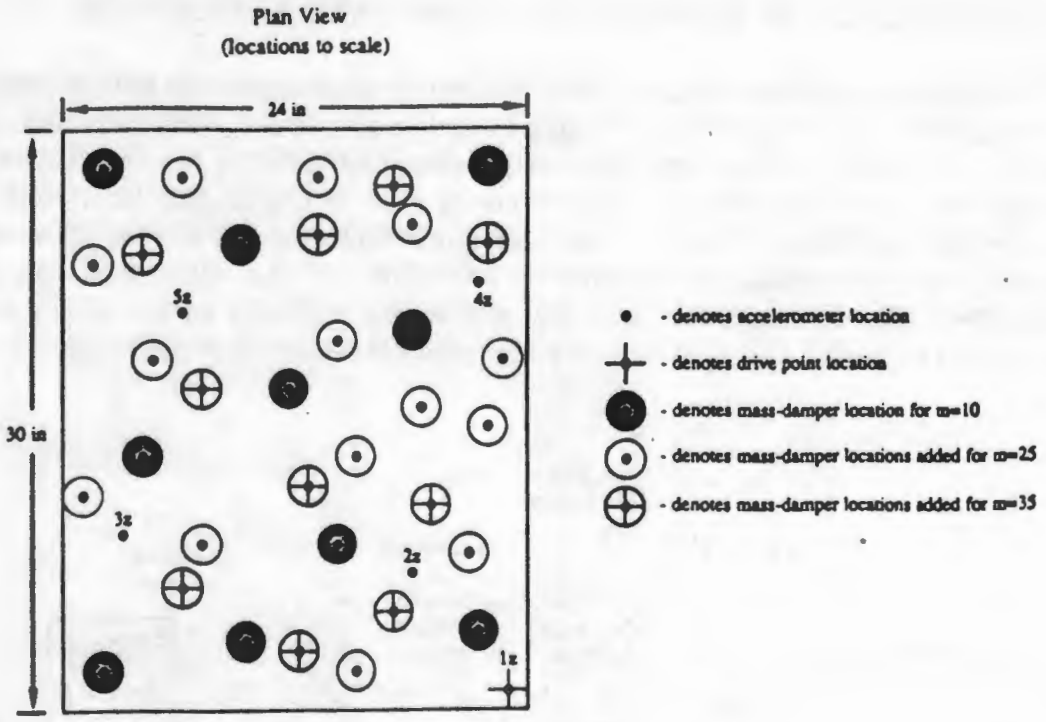

Figure 14 Accelerometer, shaker and mass-damper locations.

Table 1: Measured Plate Loss Factor η, for N=0,10,25,35						
# Mass-Dampers	Added Mass	Impedance Ratio	Center Freqs. of 320 Hz Wide Bands			
N	%	Cd/Re{Z_p}	320 Hz	960 Hz	1600 Hz	2240 Hz
None	0	N/A	0.007	0.0040	0.007	0.008
10	5	0.32	0.009	0.014	0.012	0.011
25	13	0.32	0.012	0.014	0.024	0.026
35	18	0.32	0.015	0.019	0.025	0.035

Table 2 shows the affect of large changes in the impedance ratio on the plate loss factor for a fixed quantity of mass-dampers. We would expect lower ratios to provide a larger loss factor at lower frequencies and higher ratios to provide larger loss factors at higher frequencies. In general that data on Table 2 show this trend except that we would have expected the largest impedance ratio to have the best performance in the 2240 Hz band.

Table 2: Measured Plate Loss Factor η, for N=35 Cd/Re$\{Z_p\}$=.21,.32,.94

# Mass-Dampers	Added Mass	Impedance Ratio	Center Freqs. of 320 Hz Wide Bands			
N	%	Cd/Re$\{Z_p\}$	320 Hz	960 Hz	1600 Hz	2240 Hz
35	18	0.21	0.021	0.025	0.026	0.029
35	18	0.32	0.015	0.019	0.025	0.035
35	18	0.94	0.016	0.014	0.019	0.028

Figures 15 and 16 show the average TF for the damped plate alone and the same plate with 35 mass-dampers, over frequency ranges of 10-640 Hz and 640-2540 Hz respectively. It can be seen from these curves that above 300 Hz the magnitude of the TF is reduced by as much as 15 dB.

7.0 COMPARISON ON ANALYTICAL AND EXPERIMENTAL DATA

A comparison of experimental and analytical TFs can be found on Figure 17. It can be from these curves that the analysis overestimates the TF above 1000 Hz. We also find that although the experimental and analytical data have the same trend the analysis predicts a larger reduction in the TF due to the addition of the mass-dampers than was measured experimentally. On average a 9 dB reduction is predicted while a 6 dB reduction was measured. Recent data suggests that these differences may be influenced in part by mass loading effects of the silicone bead used to contain the glycerol.

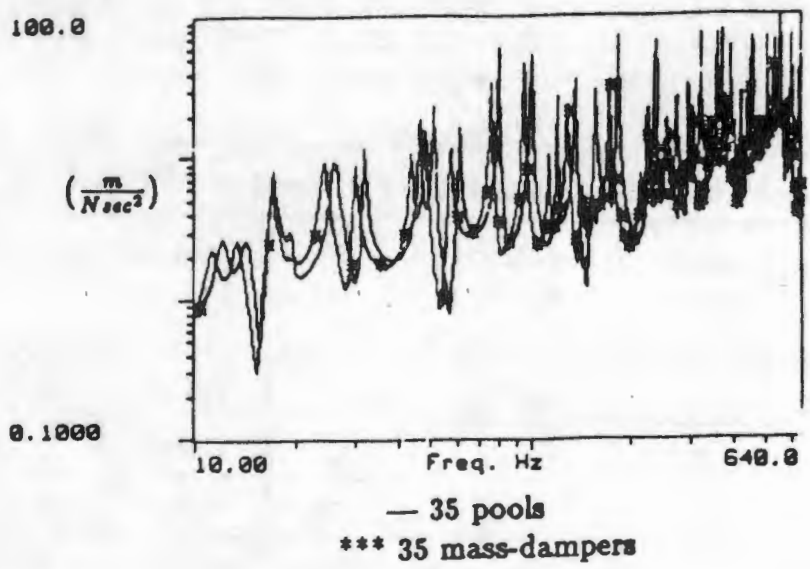

Figure 15 Comparison of average TF (10-640 Hz) for damped plate alone and damped plate with 35 mass-dampers, $C_d/Re\{Z_p\}=.32$.

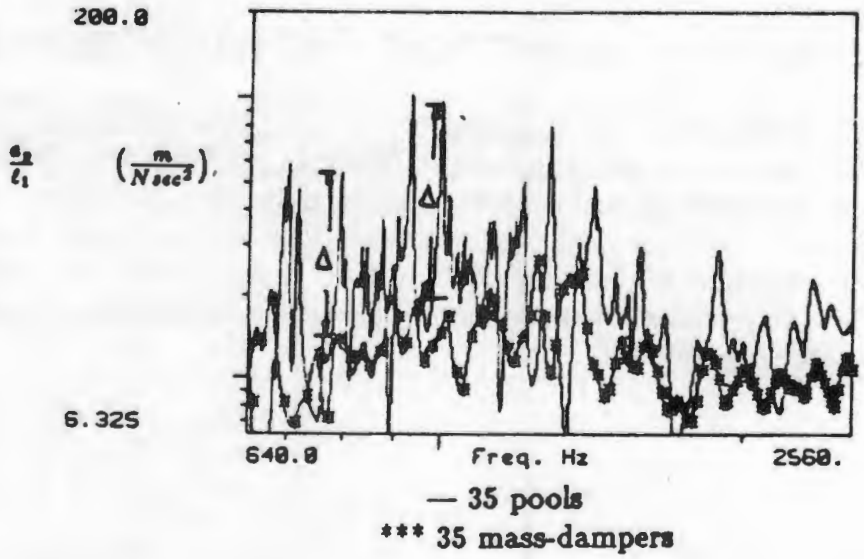

Figure 16 Comparison of average TF (640-2540 Hz) for damped plate alone and damped plate with 35 mass-dampers, $C_d/Re\{Z_p\}=.32$.

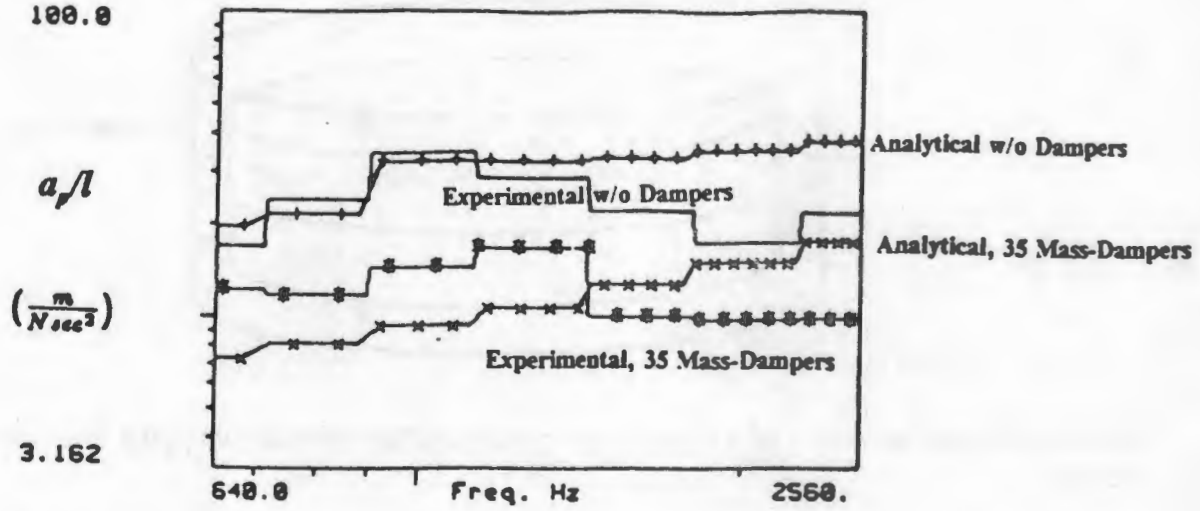

Figure 17 A Comparison of analytical and experimental average TFs with and without 35 mass-dampers.

8.0 CONCLUSIONS

SEA techniques have been used to predict the effect of impedance matched mass-dampers on the damping of a rectangular plate. This analysis indicates that plate damping can be significantly improved using this approach. The analysis also indicates that this method is most effective below 2500 Hz for the plate evaluated. Analytical work[4] done to model 3 dimensional structures as 2 dimensional ones has indicated that this approach can even be effective below 50 Hz. It appears that theoretically, there is no lower limit to the frequency at which this approach is effective, although, more mass is required to get the same effect at lower frequencies and the damping effect at higher frequencies is lessened.

A prototype impedance matched mass-damper system which utilized fluid film damping principles was built and tested. Experimental data has shown that this approach can significantly improve the damping of a plate. Because this technique does not share strain energy with the base structure but, rather looks at the base structure as a velocity source, it may prove useful in damping structures where it is difficult to design a strain energy sharing visco-elastic system. Such applications would typically be the low frequency modes of structures which generally have lower bending strain energies. Typical applications might be in marine hardware to reduce structureborne noise levels, in buildings to reduce wind and seismically induced vibrations and in automobiles or aircraft to reduce low frequency vibrations and improve passenger comfort.

A conceptual sketch of one such design is shown on Figure 18. It consists of a housing which could be made of aluminum or plastic and a hockey puck shaped mass which is softly sprung from the housing in 3 orthogonal directions.

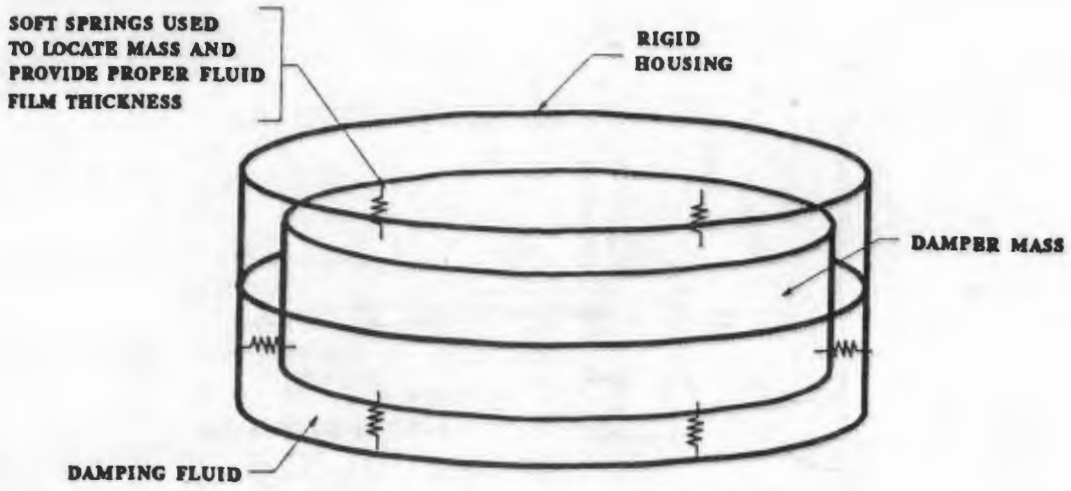

Figure 18 Conceptual sketch of a mass-damper design which provides damping in 3 orthogonal directions.

The fluid level and film thickness between the mass and housing are designed such that the system provides damping in 3 orthogonal directions, independent of its mounting orientation. This approach is the subject of a MIT patent application. Many other configurations are possible but, further work needs to be done to evaluate the design parameters required by particular appplicatons.

REFERENCES

1. Lyon, Richard H., **Machinery Noise and Diagnostics**, Butterworths Publishers, Stoneham, MA, 1987.

2. Lyon, Richard H., **Statistical Energy Analysis of Dynamical Systems: Theory and Applications**, MIT Press, Cambridge, MA 1976.

3. Lyon, Richard H., "*Statistical Analysis of Power Injection and Response in Structures and Rooms*", The Journal of the Acoustical Society of America, 45, No. 3, 545-565.

4. Gardner, Craig M., "*On the Design and Use of Impedance Matched Mass-Dampers to Reduce Structural Vibration*", MIT Dept. of Mechanical Engineering, Masters Thesis, May, 1989.

5. Peters, J., and VanHerck,P., Theory and Practice of Fluid Dampers in Machine Tools", *Advances in Machine Tool Design and Research, 1969. Proceeding of 10th International M.T.D.R. Conference*, September 1969, University of Manchester.

6. Schroeder, M. R., "New Method for Measuring Reverberation Time", *The Journal of the Acoustical Society of America, 37*, No. 3, 409-412, March, 1965.